

PROBING THE EPOCH OF PRE-REIONIZATION BY CROSS-CORRELATING COSMIC MICROWAVE AND INFRARED BACKGROUND ANISOTROPIES

F. ATRIO-BARANDELA¹, A. KASHLINSKY²

Draft version June 9, 2019

ABSTRACT

The epoch of first star formation and the state of the intergalactic medium (IGM) at that time are not directly observable with current telescopes. The radiation from those early sources is now part of the Cosmic Infrared Background (CIB) and, as these sources ionize the gas around them, the IGM plasma would produce faint temperature anisotropies in the Cosmic Microwave Background (CMB) via the thermal Sunyaev-Zeldovich (TSZ) effect. While these TSZ anisotropies are too faint to be detected, we show that the cross-correlation of maps of source-subtracted CIB fluctuations from *Euclid*, with suitably constructed microwave maps at different frequencies can probe the physical state of the gas during reionization and test/constrain models of the early CIB sources. We identify the frequency-combined CMB-subtracted microwave maps from space and ground-based instruments to show that they can be cross-correlated with the forthcoming all-sky *Euclid* CIB maps to detect the cross-power at scales $\sim 5' - 60'$ with the signal/noise of up to $S/N \sim 4 - 8$ depending on the contribution to the Thomson optical depth during those pre-reionization epochs ($\Delta\tau \simeq 0.05$) and the temperature of IGM (up to $\sim 10^4\text{K}$). Such a measurement would offer a new window to explore emergence and physical properties of these first light sources.

Subject headings: Cosmic Background Radiation. Cosmology: Observations. Dark Ages, Reionization, First Stars.

1. INTRODUCTION.

Within the framework of the standard cosmological model it is theoretically believed that the first objects in the Universe were dominated by massive stars and the first black holes which formed in minihalos of $\sim 10^6 - 10^7 M_{\odot}$ (Bromm & Yoshida 2001). These objects cannot be detected individually with present-day instruments, so alternative methods are needed to probe the epochs of first star formation.

At near-IR wavelengths (below $\sim 5\mu\text{m}$) the cosmic infrared background (CIB) probes emissions by stellar and black hole sources (Kashlinsky 2005) and its fluctuations may contain a substantial component from the first sources Kashlinsky et al. (2004); Cooray et al. (2004). Significant CIB fluctuations have been identified in *Spitzer* (Kashlinsky et al. 2005, 2007, 2012) and *Akari* (Matsumoto et al. 2011) data between ~ 2 and $\sim 5\mu\text{m}$ after known galaxy populations have been subtracted to deep levels. The fluctuations are too large and have the wrong spatial distribution to be explained by known galaxy populations (Kashlinsky et al. 2005; Helgason et al. 2012). Their origin was suggested to lie at the epoch of first stars (Kashlinsky et al. 2005, 2007) as implied by the slope of their spatial spectrum now measured to $\sim 1^{\circ}$ (Kashlinsky et al. 2012). The high- z interpretation of the residual fluctuations is supported by the observed lack of correlation between the *Spitzer* CIB fluctuations and optical *HST* image data out to $0.9\mu\text{m}$ where the Lyman-break at wavelength $0.1(1+z)\mu\text{m}$ is ex-

pected (Kashlinsky et al. 2007). The source-subtracted CIB fluctuations appear highly coherent with the soft $[0.5 - 2]\text{KeV}$ unresolved X-ray cosmic background (CXB) with no detectable coherence appearing at harder X-ray energies (Cappelluti et al. 2013). The measured correlation requires a proportion of accreting black holes among the CIB sources significantly higher than in the directly observed populations (Helgason et al. 2014), further supporting the high- z origin of these sources and inconsistent with the alternative proposal for the origin of the CIB fluctuations in intrahalo light at more recent epochs (Cooray et al. 2012, see also Sec. 4.3 of Helgason et al. 2014 for summary of further observational difficulties of this scenario).

We will assume here that the sources producing these CIB fluctuations at $(2 - 5)\mu\text{m}$ lie at early epochs, $z \gtrsim 8$, consistent with all the CIB-related measurements. This will be tested definitively with the *Euclid* data, where this team has been selected by NASA/ESA to conduct an all sky near-IR CIB program LIBRAE (Looking at Infrared Background Anisotropies with *Euclid*). At high- z , these early sources would have ionized and heated up the surrounding gas which, in principle, would generate secondary anisotropies in the Cosmic Microwave Background (CMB) via the thermal Sunyaev-Zeldovich (TSZ) effect. Given that *Euclid* will cover $\sim 20,000 \text{ deg}^2$ with sub-arcsec resolution at three near-IR channels (*Euclid* Red Book 2011) this weak signal may be teased out of the noise, after suitable construction of a comparably large-area, low noise, multifrequency CMB maps of $\sim \text{arcmin}$ resolution which are expected to be available in the near future. We show here how such measurements can lead to a highly statistically significant result for plausible modes of the high- z evolution. At the same time, if the signal originates at high- z , there should be

¹ NASA Goddard Space Flight Center, Greenbelt, MD 20771. On sabbatical leave from the University of Salamanca, Spain. Email: atrio@usal.es

² Code 665, Observational Cosmology Lab, NASA Goddard Space Flight Center, Greenbelt, MD 20771 and SSAL, Lanham, MD 20770; email: Alexander.Kashlinsky@nasa.gov

no correlation between the CMB and the diffuse emission maps obtained from the *Euclid* VIS (visible) channel. Our goal here is not to test specific models, but rather to demonstrate how the first ionization sources very generally can produce a measurable CIB×CMB signal, whose detection or upper limit can then be used to probe the emergence of the Universe out of the “Dark Ages”.

2. CIB SOURCES AND CROSS-POWER WITH CMB

The measured CIB fluctuation spectrum appears consistent with the high- z Λ CDM clustering and is the same (within uncertainties) in different sky directions consistent with its cosmological origin (Kashlinsky et al. 2012). The source-subtracted CIB fluctuations have two components: 1) shot/white noise from the remaining (unresolved) sources dominates small angular scales and sets an *upper* limit on the shot-noise of the new high- z populations, and 2) a fluctuation component due to clustering of *new* population sources is found at scales $> 20''$. We use these measurements to normalize the TSZ anisotropy to the flux from, and the abundance of, the sources at high- z using the outline similar to Kashlinsky et al. (2007).

Massive Population III stars of mass m_* would radiate at the Eddington limit with luminosity $l_* \propto m_*$. They would have approximately constant surface temperature $T_* \sim 10^5$ K and would have produced a large number of ionizing photons with energy ≥ 13.6 eV. These lead to a constant ratio of the ionizing photons per H-burning baryon in these objects. The results of Bromm et al. (2002); Schaerer (2002) give a number of ionizing photons $\mathcal{N}_i \sim 10^{62} M_*/M_\odot$ produced over the lifetime of these stars ($\sim 3 \times 10^6$ yr) by a halo containing M_* in such sources. If κ ionizing photons are required to ionize a H atom, around each halo containing M_* in stars there will be a bubble of $M_{\text{ion}} \sim 10^5 \kappa^{-1} M_*$ ionized gas, heated to a temperature of $T_e \equiv T_{e,4} 10^4$ K. Hereafter we will ignore spatial variations on κ , and assume that most photons escape from the halos where they originate; see discussions of Santos et al. (2002); Salvaterra & Ferrara (2006) for stars and Yue et al. (2013); Mesinger et al. (2013) for early black holes. If the electron temperature T_e and density n_e are constant, the Comptonization parameter averaged over the solid angle ω_B subtended by the bubble would be $Y_{C,B} = (4/3)\sigma_T n_e R_{\text{ion}}(kT_e/m_e c^2)$, where R_{ion} is the radius of the ionized cloud and m_e the electron mass. Each ionized bubble would generate a CMB mean distortion over a pixel of solid angle ω given by $t_{\text{TSZ,B}} = G_\nu Y_{C,B} \frac{\omega_B}{\omega} T_{\text{CMB}}$ where G_ν is the frequency dependence of the effect Birkinshaw (1999). The net distortion will be the added contributions of all bubbles in the CMB pixel, $T_{\text{TSZ}} = n_2 \omega t_{\text{TSZ,B}}$, where $n_2 \omega$ is the total number of bubbles along the line of sight on a pixel of solid angle ω .

Strong *lower* limits on the projected number density of sources/bubbles can be set by the combination of the measured *upper* limit on the CIB shot-noise power, P_{SN} , and the amplitude of the clustering component of the CIB fluctuations (Kashlinsky et al. 2007). Populations at high- z , which are strongly biased and span a short period of cosmic time, are expected to produce $\Delta \sim 10\%$ relative CIB fluctuations on arcmin scales requiring a net flux of $F_{\text{CIB}} = \delta F_{\text{CIB}}/\Delta \sim 1$

nW/m²/sr from these populations. At the same time, since $P_{\text{SN}} \sim F_{\text{CIB}}^2/n_2$, the measured *upper* limit of $P_{\text{SN}} \simeq 10^{-11}$ nW²/m⁴/sr (Kashlinsky et al. 2007) implies a *lower* limit on the 2-D angular sky density of these sources of $n_2 \gtrsim 10^{11}$ sr⁻¹ $P_{\text{SN},-11}^{-1}$ with $P_{\text{SN}} \equiv P_{\text{SN},-11}^{-1} 10^{-11}$ nW²/m⁴/sr being the shot-noise power of the high- z sources. Then,

$$T_{\text{TSZ}} \simeq \frac{4}{\pi} G_\nu T_{\text{CMB}} \frac{k_B T_e \sigma_T}{m_e c^2} \frac{M_{\text{ion}}}{d_A^2} \frac{F_{\text{CIB}}^2}{\mu m_H P_{\text{SN}}} \simeq 200 G_\nu \left(\frac{0.5 \text{Gpc}}{d_A} \right)^2 \frac{M_*}{10^4 \kappa \mu M_\odot} T_{e,4} \frac{F_{\text{CIB}}^2}{P_{\text{SN},-11}} \text{nK} \quad (1)$$

Here, F_{CIB} is the net CIB flux from these sources in nW/m²/sr, μ is the mean gas molecular weight and k_B the Boltzmann constant. M_* corresponds to a conservative choice for the mass of the ionizing sources in each early halo. In standard cosmology $d_A = 0.5\text{--}0.9$ Gpc at $z = 20\text{--}10$. For the above parameters, eq. 1, the effective Thomson optical depth due to the reionized medium is $\tau_{\text{eff}} \equiv 200 \text{nK} / [T_{\text{CMB}}(k_B T_e / m_e c^2)] = 0.044$, well below the measured value of $\tau = 0.097 \pm 0.038$ (Planck Collaboration 2013).

Due to the variation on the number density of bubbles with a relative number fluctuation of $\Delta \simeq 0.1$ (Kashlinsky et al. 2007), the CMB distortion T_{TSZ} would generate CMB temperature fluctuations. If we further assume that the ionized bubbles are distributed as the halos where the ionized photons originate, the TSZ temperature anisotropies would have an amplitude $\sim T_{\text{TSZ}} \Delta$ that could potentially be detected by cross-correlating the produced CMB anisotropies with CIB fluctuations. If P_{CIB} , P_{TSZ} and $P_{\text{CIB} \times \text{TSZ}}$ are the power spectrum of the CIB flux, TSZ anisotropies and their cross-power, respectively, the coherence between CIB sources and bubbles is $C = P_{\text{CIB} \times \text{TSZ}}^2 / (P_{\text{CIB}} P_{\text{TSZ}})$. For bubbles coherent with CIB sources ($C \simeq 1$), the cross-power between CIB and TSZ is $P_{\text{CIB} \times \text{TSZ}} \simeq \sqrt{P_{\text{CIB}}} \sqrt{P_{\text{TSZ}}}$. To compute this cross-correlation, the sub-arcsec *Euclid* CIB and arcmin-resolution CMB maps will be brought to a common resolution. When measuring the cross-power from IR and microwave maps (μ) of N_{pix} CMB pixels, the error is $\sigma_{P_{\text{CIB} \times \text{TSZ}}} \simeq \sqrt{P_{\text{IR}}} \sqrt{P_\mu} / \sqrt{N_{\text{pix}}}$ (Kashlinsky et al. 2012; Cappelluti et al. 2013). At the scales of interest here ($\gtrsim 1'$) the *Euclid* CIB maps will have negligible noise, so $P_{\text{IR}} = P_{\text{CIB}}$. Using the *Euclid* Wide Survey of $\mathcal{A} \simeq 20,000 \text{deg}^2$ the CIB power on arcmin scales will be measurable by LIBRAE down to sub-percent statistical accuracy. If primary CMB is removed, the foreground-reduced microwave maps would be dominated by instrument noise σ_n , foreground residuals $\sigma_{f, \text{res}}$ and, more importantly, the TSZ of the unresolved cluster population $\sigma_{\text{unr}, cl}$. With N_ν frequency channels the variance of the microwave map would be $\sigma_\mu^2 = \sigma_n^2 / N_\nu + \sigma_{f, \text{res}}^2 + \sigma_{\text{unr}, cl}^2$. The signal-to-noise would be $S/N \simeq T_{\text{TSZ}} \Delta \sqrt{N_{\text{pix}}} / \sigma_\mu$, which can reach $S/N \gg 1$ for some experimental configurations discussed below. Specifically

$$S/N = 7 \frac{T_{\text{TSZ}}}{200 \text{nK}} \frac{\Delta}{0.1} \frac{5 \mu\text{K}}{\sigma_\mu} \left(\frac{N_{\text{pix}}}{3 \times 10^6} \right)^{\frac{1}{2}}, \quad (2)$$

where $N_{\text{pix}} = 3 \times 10^6$ corresponds to 20,000 deg² binned into independent squares of 5' on the side, the expected sky coverage of the *Euclid* satellite downgraded to the native resolution of *Planck*.

3. CMB DATA

Eq. 2 shows that CMB maps with low σ_μ covering a sufficiently large sky area are needed for a statistically significant measurement of the CIB×TSZ cross correlation. Such maps already exist and more will be available in time for the upcoming *Euclid* CIB measurement with LIBRAE. Resolved sources in *Spitzer* CIB analysis remove $\sim 25\%$ of the sky (Kashlinsky et al. 2005, 2012); this fraction is expected to be lower for the much better resolution of *Euclid*, which in any event will then be pixelated into the CMB resolution of \gtrsim arcmin.

To transform these CMB data into maps suitable for probing the contribution of the TSZ from the first stars era and gain insight into the epochs prior to completion of the reionization, one needs to remove the primary CMB component of $\sigma_{\text{CMB}} \sim 80\mu\text{K}$, which is feasible with the multi-frequency microwave maps obtained, and obtainable, with numerous instruments by, for example, subtracting a 217GHz map, the null of the TSZ effect, from maps at other frequencies. In this process other black-body components, such as from the integrated Sachs-Wolfe and kinetic SZ effects, will also be removed. After the suitable CMB subtraction has been achieved the microwave maps will be cross-correlated, via the cross-power (see Kashlinsky et al. 2012; Cappelluti et al. 2013), with the *Euclid* CIB maps to be produced over patches of $\sim 1^\circ$ on the side and covering 20,000 deg² in the *Euclid* Wide Survey. We now specify several instrumental configurations for such a measurement.

- *Planck*. For *Planck* channels at frequencies $\nu = (100, 143, 217, 353)\text{GHz}$, the beams have an effective FWHM=(9.65, 7.25, 4.99, 4.86)' (Planck Collaboration 2013). At these frequencies $G_\nu = (-1.51, -1.04, 0., 2.23)$ and the noise after the planned two years of integration is $\sigma_n = [1.3, 0.5, 0.7, 2.5]\mu\text{K}$ on pixels of 1° side. Other contributions to the overall σ_μ come from sources below the threshold detection level of the instrument. The amplitude of the Poisson and clustered foreground power spectra $D_\ell = \ell(\ell+1)C_\ell/2\pi$ at $\ell = 3000$ are $A^{PS} = (220 \pm 53, 75 \pm 8, 60 \pm 10)\mu\text{K}^2$ and $A^{CL} = (\sim 0, 32 \pm 8, 50 \pm 5)\mu\text{K}^2$ for 100, 143 and 217GHz, after 1 yr of integration (Planck Collaboration 2013). The Planck Collaboration does not provide values of these contributions at 353GHz, so we will assume them to be negligible. These components will not cancel when subtracting the 217GHz map from those of other frequencies. The TSZ from unresolved clusters has an amplitude $A^{TSZ} = 4G_\nu^2\mu\text{K}^2$, that will also be present (Planck Collaboration 2013). In summary, the noise in the *Planck* CMB difference maps $\nu - 217\text{GHz}$ is $\sigma_{\nu-217\text{GHz}} = (9.6, 10.3, 32.0)\mu\text{K}$ for $\nu = (100, 143, 353)\text{GHz}$ on pixels corresponding to the FWHM at each frequency. Combining the three channels, taking into account the frequency dependence of the TSZ effect, the error on the Comptonization parameter would be $\sigma_\mu^{\text{Planck}} = 7.8\mu\text{K}$ on pixels of 5' after 2 yrs.

- *The Atacama Cosmology Telescope* (ACT) has already mapped CMB over 600deg² at 148, 218 and

277GHz with resolution (1.4', 1.0', 0.9') (Gralla et al. 2013). The currently observed area is small for the purposes of the present discussion and adds little to the S/N of the measurement, but an expanded area could eventually provide useful data.

- *South Pole Telescope* (SPT) has already mapped 2,540 deg² at (95, 150, 220)GHz, with resolution (1.7, 1.2, 1.0)'. The noise levels are 18 μK at 150GHz and $\sim \sqrt{2}$ larger for the other two channels (George et al. 2014). The CMB-subtracted maps have a residual noise of $\sigma_{\nu-220\text{GHz}} \simeq (36, 32)\mu\text{K}$ with a similar number of pixels as Planck ($N_{\text{pix}} > 3 \times 10^6$) for the lowest resolution channel. Combining the two frequencies, the noise on the Comptonization parameter scaled to 5' pixels is $\sigma_\mu^{\text{SPT}} = 4.74\mu\text{K}$, smaller than that of Planck but over 1/8 the area covered by *Euclid*. It would provide competitive results with those of *Euclid* and *Planck*. In addition, due to its location, the SPT data should be useful for a similar analysis with WFIRST (Spergel et al. 2013).

- *Future experiments* like Advanced ACT and CMB-Stage 4 (Abazajian et al. 2014) would aim to map 1/2-2/3 of the sky with sensitivity of $\sim 10\mu\text{K}/\text{arcmin}$ and $\sim 1\mu\text{K}/\text{arcmin}$ at a wide range of frequencies, 30-300GHz and 40-240GHz, respectively. In these future instruments, the limiting factor will not be instrumental noise, but confusion from foreground sources and TSZ contributions from unresolved clusters. These foregrounds would contribute $\sigma_{\text{for}} \sim 3 - 10\mu\text{K}$ in the frequency range 100-217GHz. These low noise levels, in combination with *Euclid* and, potentially also WFIRST-based, CIB maps, offer the exciting possibility of probing how CIB sources affected the physical properties of the IGM prior to reionization.

4. THE CIB-CMB CROSS POWER SPECTRUM

We can refine the previous estimate (eq. 2) by a specific model computation of the cross-power of TSZ anisotropies and CIB fluctuations. We compute the TSZ-CIB cross-power on angular scale $\theta = 2\pi/q$ via the relativistic Limber equation

$$P_{\text{CIB} \times \text{TSZ}}(q) = \int dr(z) \left(\frac{dF_{\text{CIB}}}{dr} \right) \left(G_\nu \frac{dY_C}{dr} \right) \frac{P_3(q/r, z)}{r^2}, \quad (3)$$

and normalize it to the *measured* CIB auto-power as discussed in (Kashlinsky et al. 2014). In the above, $q = 2\pi/\theta$, P_3 is the 3-D biased power spectrum of the sources, and $r(z) = d_A(1+z) = d_L/(1+z)$ is the comoving distance.

As in Kashlinsky et al. (2004), we assume that the sources radiate at the Eddington limit, form proportionally to their collapse rate and, in addition, are designed to reproduce the measured *integrated* CIB fluctuations over (2-5) μm , verifying that their relative fluctuation $\Delta \simeq 0.1$ at $2\pi/q = 5'$ (Kashlinsky et al. 2014). As the ionized bubbles appear around the CIB sources, they will start generating the optical depth due to Thomson scattering, $d\tau/dr = \rho_{\text{baryon}}/(\mu m_p)\sigma_T x_e(1+z)^{-1}$ where x_e is the ionization fraction, as well as contribute to the Comptonization, $dY_C/dr = (k_B T_e/m_e c^2)d\tau/dr$. Because the ionized bubbles surround the first sources, we assume the same biasing for both TSZ and CIB and use the methodology of Kashlinsky et al. (2004); Cooray et al. (2004) to relate

it to the underlying standard Λ CDM power spectrum.

In principle, the ionization fraction $x_e(z)$ can be related to fraction of baryons in stars as: $x_e = n_I f_*$, where n_I is the number of ionized atoms per baryon in CIB sources and $f_*(z)$ is the fraction locked in CIB sources up to z . To simplify our treatment, we parametrize $f_*(z) \propto \text{erfc}((z - z_0)/\Delta z)$ where z_0 is the redshift at which half of f_* have been locked up in CIB sources, Δz determines how fast baryons collapse to form CIB sources. We normalize below to the overall optical depth produced by these sources $\Delta\tau = 0.05$ and take the temperature of the gas in the bubbles to be $T_e = 10^4\text{K}$, where atomic cooling becomes inefficient in the absence of H_2 . In the presence of heating by accreting black holes or X-ray binaries, T_e can rise somewhat above 10^4K (Mirabel et al. 2011; Jeon et al. 2014).

We assumed in computations that $z_0 = [13, 20]$ and $\Delta z = [0.3, 1.3]$ fixing the final ionization fraction to reproduce $\Delta\tau = 0.05$; this corresponds to $0.3 < x_e < 1$ at the end of that period. We verify that the coherence of these models varies between $0.8 < \sqrt{C_{\text{TSZ} \times \text{CIB}}} < 0.95$ to compare with the discussion in Sec. 2. In Fig 1a we show how the optical depth reaches $\Delta\tau = 0.05$ for these models. Fig 1b shows S/N with which the experiments discussed in Sec. 3 can probe the CIB \times TSZ cross-correlation at different angular scales. We always assume that the experiment has at least two frequencies with overlapping resolution so the primary CMB and the kinetic SZ component can be removed from the maps. The band width encloses the minimum/maximum values of all our models. Notice that the final S/N is weakly dependent on when reionization occurs (parametrized by z_0) and the width of this period (Δz). This is a consequence of normalizing all models to the measured CIB flux and to the same electron optical depth. The blue band corresponds to an experiment with the instrumental noise and foreground residuals of $\sigma_{\text{noise}} = 5\mu\text{K}$ on pixels of $5'$ side covering the area of the *Euclid* wide field survey. The red band corresponds to the S/N using *Euclid* and the HFI *Planck* data at the end of the nominal 2yr mission. The S/N is ~ 2 when using the 353GHz and 217 GHz channels and increases to ~ 5 when the 143 and 100 GHz channels are added. Adding SPT data (George et al. 2014) increases the S/N to ~ 6 at $13'$.

The results of Fig 1 scale as $(S/N) \propto \Delta\tau \cdot T_e$ lead-

ing to higher significance for $T_{e,4} > 1$ as reached in e.g. modeling of Jeon et al. (2014). The S/N can be increased by computing the cross-power over wider angular bins allowing to probe much lower parameters as done in Cappelluti et al. (2013). In addition, in experiments such as *Planck*, observing at frequencies above and below the TSZ null frequency, the CIB-TSZ correlation will change sign, offering a potential test to eliminate spurious contributions.

5. DISCUSSION

We have demonstrated that the cross-correlation of the future CIB *Euclid* maps with the CMB data expected by that time can probe or constrain the pre-reionization epochs as the Universe emerges out of the ‘‘Dark Ages’’. If 1) these sources contributed about half of the measured optical depth to the last scattering surface and 2) the ionized blobs contained gas at $T_e = 10^4\text{K}$, the measurement would be at $S/N > 6$ using the CMB map differencing method discussed here. The cross-power measurement can be further improved by computing the latter in wider angular bins. The overall S/N demonstrated here is large enough for the detection to remain significant even if parts of the *Euclid* CIB maps are polluted by Galactic cirrus, which would not correlate with the TSZ component.

At fixed angular resolution the significance scales with the area of CIB-CMB overlap, A , as $S/N \propto \sqrt{A}$. Additionally, WFIRST, the Dark Energy mission currently considered by NASA, could likewise provide significant results with its coverage of four near-IR channels currently planned to cover $\simeq 2,000\text{deg}^2$ (Spergel et al. 2013) combined with the proposed CMB-Stage 4 arcmin-resolution instrument (Abazajian et al. 2014). The planned absence of the visible channel onboard WFIRST in testing the high- z origin of the cross-power can be compensated with the *Euclid* VIS data.

Acknowledgements: NASA’s support to the LIBRAE project (PI, A. Kashlinsky) NNN12AA01C is gratefully acknowledged. FAB acknowledges financial support from the Spanish Ministerio de Educación y Ciencia (project FIS2012-30926). We thank Eric Switzer for useful information on current and future CMB experiments and Rick Arendt and Ed Wollack for comments on the draft manuscript.

REFERENCES

- Abazajian, K.N., et al, 2014, preprint arXiv:1309.5383
 Birkinshaw, M. 1999, Phys. Rep., 310, 97
 Bromm, V., Kudritzki, R. & Loeb, A. 2001, ApJ, 552, 464
 Bromm, V., Yoshida, N. 2011, ARA&A, 49, 373
 Cappelluti, N. et al. 2013, ApJ, 769, 68
 Cooray, A., Bock, J., Keating, B., Lange, A., Matsumoto, T. 2004, ApJ, 606, 611
 Cooray, A., et al. 2012, Nature, 490, 514
 Euclid Red Book:
<http://sci.esa.int/euclid/48983-euclid-definition-study-report-esa-sre-2014-12/>
 George, E.M. et al. 2014, preprint arXiv:1408.3161
 Gralla M. B. et al., 2013, preprint arXiv:1310.8281
 Helgason, K. et al. 2012, ApJ, 752, 113
 Helgason, K. et al. 2014, ApJ, 785, 38
 Jeon, M., Pawlik, A., Bromm, V. & Milosavlevic, M. 2014, MNRAS, 440, 3778
 Kashlinsky, A. 2005, Phys. Rep., 409, 361
 Kashlinsky, A., Arendt, R., Gardner, J., Mather, J., Moseley, S. H. 2004, Ap.J., 608, 1
 Kashlinsky, A., Arendt, R. G., Mather, J. & Moseley, S. H. 2007, ApJ, 654, L5
 Kashlinsky, A., Arendt, R. G., Mather, J. & Moseley, S. H. 2007a, ApJ, 654, L5
 Kashlinsky, A., Arendt, R. G., Mather, J. & Moseley, S. H. 2007, ApJ, 654, L1
 Kashlinsky, A., Arendt, R. G., Mather, J. & Moseley, S. H. 2007, ApJ, 666, L1
 Kashlinsky, A. et al. 2012, ApJ, 753, 63
 Kashlinsky, A. et al. 2014, ApJ
 Matsumoto, T. et al. 2011, ApJ, 742, 124
 Mesinger, A., Ferrara, A., & Spergel, D. 2013, MNRAS, 431, 621
 Schaerer, D. 2002, A&A, 382, 28
 Salvaterra, R., & Ferrara, A. 2006, MNRAS, 367, L11
 Santos, M., Bromm, V. & Kamionkowski, M. 2002, MNRAS, 336, 1082
 Yue, B., Ferrara, A., Salvaterra, R., & Chen, X. 2013, MNRAS, 431, 383

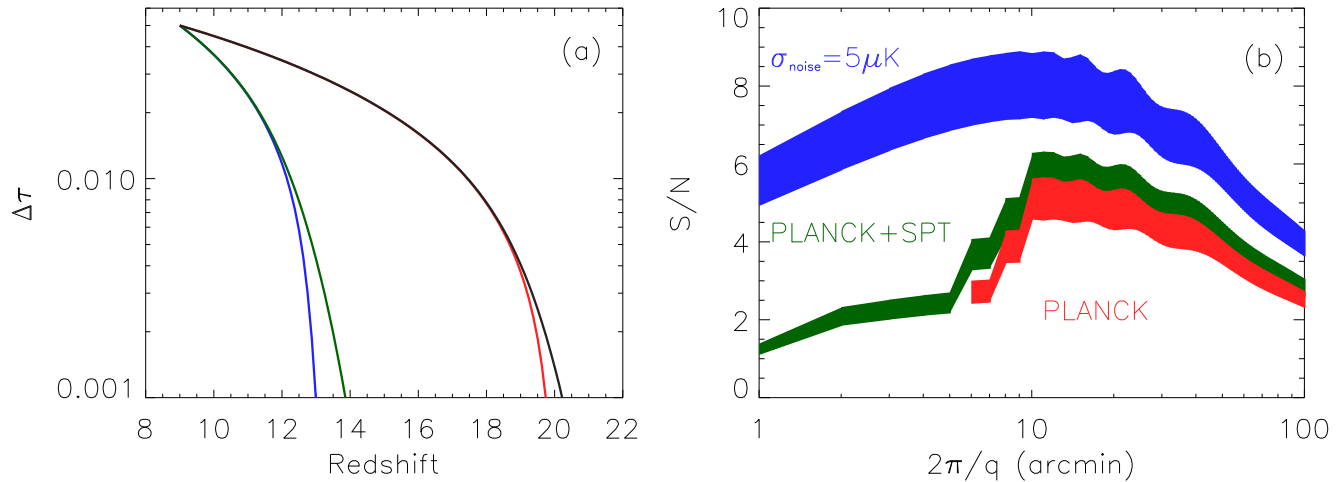


FIG. 1.— (a) The build-up of $\Delta\tau$ for the models considered here. Blue/green lines correspond to $\Delta z = 0.3/1.3$ and $z_0 = 13$, and red/black to $\Delta z = 0.3/1.3$ and $z_0 = 20$. (b) Filled regions show the range of the S/N of the CIB-TSZ cross power over the *Euclid* Wide Survey region covered by the model parameters for different experimental configurations. *Planck* parameters are projected to 2 yrs of integration and include terms discussed in Sec. 3. At $5'$ only 353–217 GHz difference maps would be useful, at $7'$ we also add 143–217 GHz, and at $> 9'$ we can add the data from 100–217 GHz. SPT has lower S/N, but can probe angular scales as low as $\sim 1'$. In its current configuration the ACT does not add appreciably to the measurement, but that can be improved with Advanced ACT and CMB Stage 4 experiments as shown with the blue band.

Planck Collaboration, Planck 2013 results. XVI. Cosmological parameters, 2013, preprint arXiv:1303.5076
 Mirabel, I. F. et al., 2011, A&A, 528, A149

Planck Collaboration, Planck 2013 results. VI. HFI data processing, 2013, preprint arXiv:1303.5067
 Planck Collaboration, Planck 2013 results. XV. CMB power spectra and likelihood, 2013, preprint arXiv:1303.5075
 Spergel, D. et al, 2013, arXiv:1305.5425